JACS
JOURNAL OF THE AMERICAN CHEMICAL SOCIETY

ARTICLE

pubs.acs.org/JACS

Dianthra[2,3-*b*:2′,3′-*f*]thieno[3,2-*b*]thiophene (DATT): Synthesis, Characterization, and FET Characteristics of New π-Extended Heteroarene with Eight Fused Aromatic Rings

Kazuki Niimi,[†] Shoji Shinamura,[†] Itaru Osaka,[†] Eigo Miyazaki,[†] and Kazuo Takimiya*[,†,‡]

[†]Department of Applied Chemistry, Graduate School of Engineering, Hiroshima University, Higashi-Hiroshima 739-8527, Japan
[‡]Institute for Advanced Materials Research, Hiroshima University, Higashi-Hiroshima 739-8530, Japan

Supporting Information

ABSTRACT: A novel highly π-extended heteroarene with eight fused aromatic rings, dianthra[2,3-*b*:2′,3′-*f*]thieno[3,2-*b*]thiophene (DATT), was selectively synthesized via a newly developed synthetic strategy, fully characterized by means of single crystal X-ray structural analysis, and examined as an organic semiconductor in thin film transistors. Even with its highly extended acene-like π-system, DATT is a fairly air-stable compound with IP of 5.1 eV. Single crystal X-ray structural analysis revealed its planar molecular structure and the lamella-like layered structure with typical herringbone packing. Theoretical calculations of the solid state electronic structure based on the bulk single crystal structure suggest that DATT affords almost comparable intermolecular orbital couplings between HOMOs (t_{HOMO}) with those of dinaphtho[2,3-*b*:2′,3′-*f*]-thieno[3,2-*b*]thiophene (DNTT), implying its good potential as an organic semiconductor for organic field-effect transistors. In fact, field-effect mobilities as high as 3.0 $cm^2 V^{-1} s^{-1}$ were achieved with vapor-processed DATT-based devices, which is comparable with that of DNTT-based devices. The molecular ordering of DATT in the thin film state, however, turned out to be not completely uniform; as elucidated by in-plane and out-of-plane XRD measurements, the face-on molecular orientation was contaminated in the edge-on orientation, the former of which is not optimal for efficient carrier transport and thus could limit the mobility.

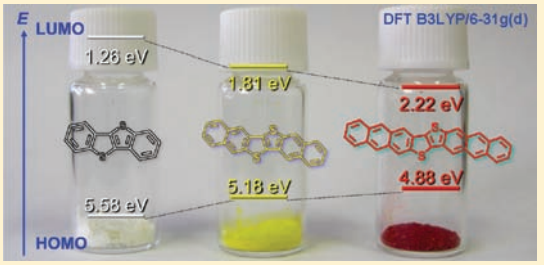

INTRODUCTION

Organic field-effect transistors (OFETs) using π-conjugated molecules or polymers as the active semiconducting layer have been intensively investigated as key elements for realizing flexible, large area electronic devices in future.[1] Recent advances in material developments as well as processing optimizations have achieved superior performances of OFETs to the amorphous silicon-based thin film transistors currently industrialized, and a mobility benchmark as high as 5.5 $cm^2 V^{-1} s^{-1}$ was reported for OFETs with polycrystalline thin films of a conventional organic semiconductor, pentacene consisting of five fused benzenes.[2] The high performance of the pentacene-based OFETs is generally interpreted by its small reorganization energy (λ) at the molecular level and large intermolecular electronic couplings (transfer integrals, t) at the solid-state level.[3] With extension of π-conjugation system, λ tends to decrease, whereas t increases,[3] and thus much larger acenes than pentacene are expected to be better organic semiconductors. Large acene molecules such as pentacene, however, have a drawback of poor air-stability owing to their high-lying HOMO energy levels.[4] Moreover, hexacene and heptacene,[5,6] higher homologues in the acene series, are not just air-unstable but chemically labile; they are readily involved in chemical reactions such as Dield−Alder-like cycloaddition and homodimerization.[7] Thus, even for isolation of such higher acenes, it is necessary to introduce bulky substituents for the steric protection from these chemical reactions (Figure 1).

To circumvent the instability of the higher acenes, structurally related π-extended, ladder-type compounds with much better stability have been focused; such compounds are oligothienoacenes with up to eight thiophene rings,[8] heteroaromatic-benzene-alternating systems with up to nine aromatic rings (Figure 1).[9] Although their stabilities are fairly improved thanks to the incorporated heteroaromatic rings, solubilizing substituents are necessary to keep the synthetic intermediates and the products soluble, in particular, for largely extended compounds more than seven fused rings. Their packing and solid-state electronic structures are thus largely altered by the substituents, which makes it unclear how π-extension can contribute to the transport characteristics in the solid state. To our best knowledge, dibenzo-fused [5]thienoacene with seven aromatic rings and its selenophene analogue are among the largest systems whose crystal structures and transport properties were investigated.[10]

We have recently focused on diacene-fused thieno[3,2-*b*]-thiophenes, e.g., [1]benzothieno[3,2-*b*]benzothiophene (BTBT)[11] and dinaphtho[2,3-*b*:2′,3′-*f*]thieno[3,2-*b*]thiophene (DNTT),[12] as stable π-extended molecular frameworks for the development

Received: March 16, 2011
Published: April 30, 2011

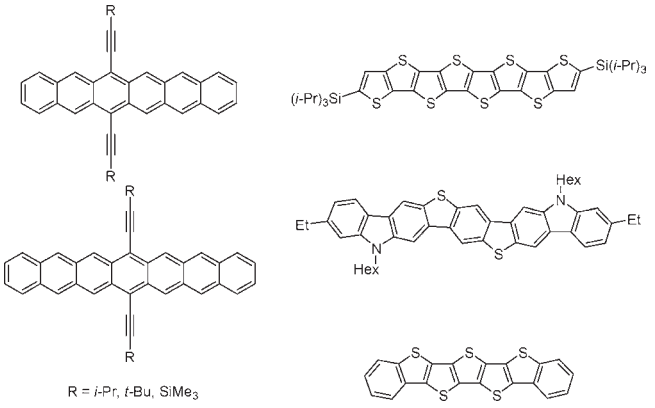

Figure 1. Largely π-extended ladder-type compounds.

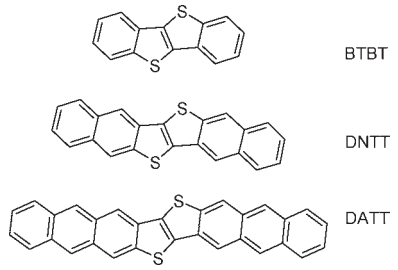

Figure 2. Chemical structures of diacene-fused thieno[3,2-*b*]-thiophenes.

of organic semiconductors (Figure 2). In fact, the BTBT and DNTT derivatives are quite useful for the development of high-performance OFETs and their integrated devices and circuits.[13,14] In particular, the parent DNTT-based OFETs show mobilities as high as 3.1 $cm^2 V^{-1} s^{-1}$ for thin film transistors[12] and 8.3 $cm^2 V^{-1} s^{-1}$ on single crystals.[15] Furthermore, alkylated DNTT derivatives show much enhanced mobilities in vapor-deposited thin film transistors (up to 7.9 $cm^2 V^{-1} s^{-1}$)[16a] and solution-processed single-crystalline film transistors (up to 12 $cm^2 V^{-1} s^{-1}$).[16b] Although the DNTT core has a highly π-extended arene structure consisting of six fused aromatic rings, the molecules are very stable, thanks to the thieno[3,2-*b*]thiophene moiety embedded in the middle of two naphthalenes.[17] For further material development along this structural motif, we have been interested in an anthracene-integrated molecule, dianthra[2,3-*b*:2′,3′-*f*]thieno[3,2-*b*]thiophene (DATT, Figure 2) with *eight* fused aromatic rings.

In this article, we report a straightforward synthesis of DATT featuring a newly developed selective functionalization of anthracene at the 2 and 3 positions and the molecular and packing structure, solid-state electronic structure, and thin film transistor characteristics of DATT.

RESULTS AND DISCUSSIONS

Synthesis. We first attempted to synthesize DATT using the same synthetic methodology as for the DNTT derivatives[12,16a] starting from anthracene-2-carbaldehyde (**1**) (Scheme 1).[8,19] The first methylthiolation reaction on **1** gave a mixture consisting of desired 3-methylthioanthracene-2-carbaldehyde (**2**) and its 1-methylthio isomer (**2′**) (80% yield as an isomer mixture). Although isolation of **2** was attempted by chromatography and/or fractional recrystallization, their poor solubility and

Scheme 1. Attempted Synthesis of DATT from Anthracene-2-carbaldehyde (1)

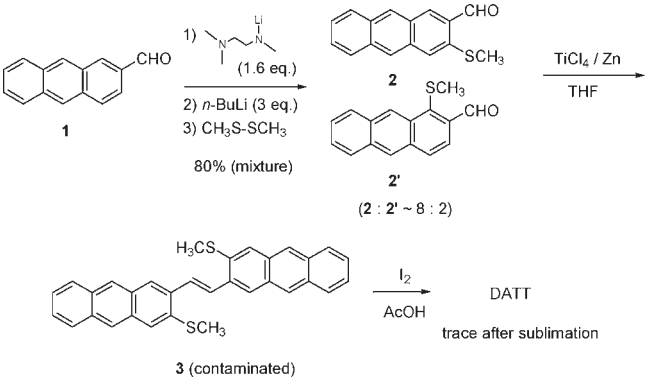

Scheme 2. Successful Synthesis of DATT

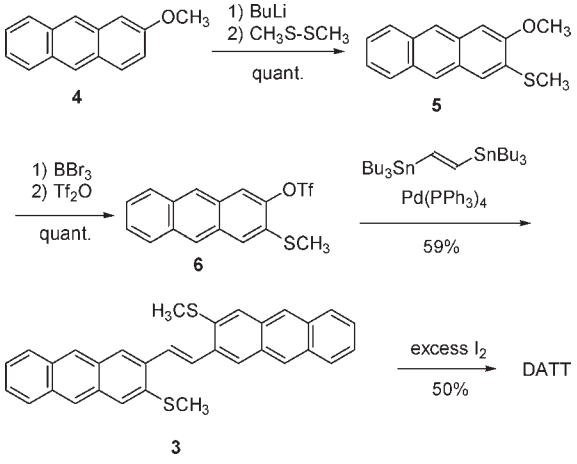

similar crystallinity prevented complete isolation, resulting in ca. 80% pure **2** at best. Thus, the sample was resignedly used in the following low-valent titanium mediated coupling reaction, which gave a mixture of the corresponding ethenes containing the precursor of DATT, *trans*-1,2-bis(3-methylthioanthracen-2-yl)ethene (**3**). Isolation of **3** from the mixture by fractional recrystallization and/or chromatography failed owing again to the poor solubility. The final ring-closing reaction using the isomeric ethenes gave a complex mixture, sublimation of which afforded only a trace amount of DATT contaminated with other isomer(s). We therefore concluded that this approach is not realistic for synthesizing DATT effectively.

To circumvent the poor selectivity of 3-functionalization on **1**, we have examined various potential routes and finally found a straightforward synthetic methodology (Scheme 2); starting from 2-methoxyanthracene (**4**),[20] 3-methylthiolation was selectively achieved to give **5** quantitatively, and the 2-methoxy functionality of **5** was utilized as a handle for introducing the ethene moiety. After selective demethylation of the methoxy group keeping the methylthio moiety intact, the resulting alcohol was readily converted into triflate **6**, which was then utilized in the palladium-catalyzed Stille coupling reaction with 1,2-bis(tributylstannyl)ethene to give the precursor of DATT (**3**).[21] The final ring-closing reaction constructing the

dx.doi.org/10.1021/ja202377m |*J. Am. Chem. Soc.* 2011, 133, 8732–8739

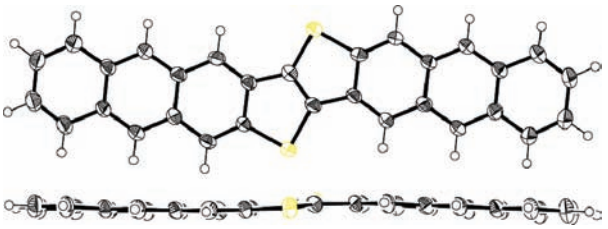

Figure 3. Molecular structure of DATT.

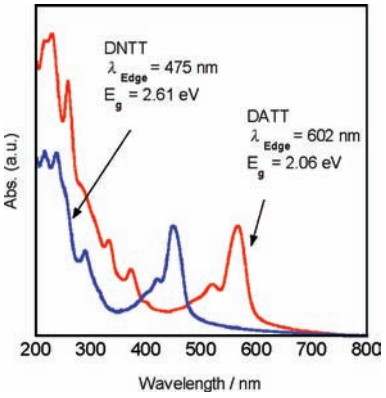

Figure 4. Absorption spectra of thin films of DNTT and DATT.

central thieno[3,2-*b*]thiophene moiety promoted by excess iodine was smoothly proceeded to afford DATT. Note that this simple synthesis is highly selective, affording good yield in each step, and thus quite efficient for constructing largely π-conjugated ladder-type compounds with the thieno[3,2-*b*]thiophene moiety.

DATT was a stable, dark-red compound and readily purified by vacuum sublimation. Owing to its poor solubility, characterization of DATT was done by mass spectroscopy and combustion elemental analysis. The structure was unambiguously confirmed by single crystal X-ray analysis, which clearly shows its rigid and planar molecular structure (Figure 3).

Physicochemical Properties and MO Calculations. As expected from its highly extended, planar structure, solubility of DATT is too low to evaluate its electrochemical properties and absorption spectra in solution. Instead, we measured ionization potential (IP) of its evaporated thin film with photoelectron yield spectroscopy in air (PESA), and the IP of DATT was determined to be 5.1 eV (Figure S1 in Supporting Information), which agrees well with the value predicted from the theoretical calculations (vide infra). Comparison of the IP value to those of BTBT (5.8 eV) and DNTT (5.4 eV) indicates that extension of π-framework certainly elevates the HOMO energy level. However, DATT still keeps a relatively low-lying HOMO energy level sufficient for air stability.[22] The absorption spectra of the DATT thin film shown in Figure 4 represents similar but bathochromically shifted absorption bands compared to that of DNTT, reflecting its smaller HOMO−LUMO gap (E_g). Estimated E_gs from the absorption edge are ca. 2.61 eV for DNTT and 2.06 eV for DATT, respectively. These values are much larger than the E_g of the hexacene derivative (Figure 1) estimated from its solution absorption spectra (~1.36 eV),[5] reflecting the phene-like electronic structure of DATT at the central thieno[3,2-*b*]thiophene moiety.[17]

These physicochemical properties of DATT are well reproduced by theoretical MO calculations.[23] The HOMO energy

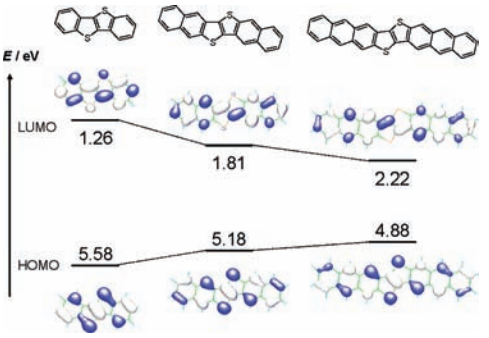

Figure 5. Calculated frontier orbitals of BTBT, DNTT, and DATT at the DFT B3LYP/6-31 g(d) level.

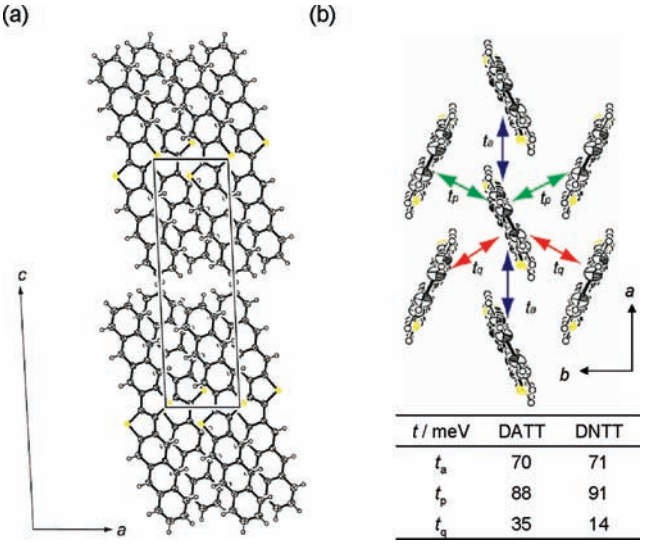

t / meV	DATT	DNTT
t_a	70	71
t_p	88	91
t_q	35	14

Figure 6. (a) Crystal structure (*b*-axis projection) and (b) packing structure in the crystallographic *ab* cell with calculated intermolecular HOMO couplings (transfer integrals of HOMO; *t*HOMO) of DATT together with t_{HOMO} of DNTT.

level of DATT estimated from the MO calculations (Figure 5) is higher by ca. 0.3 eV than that of DNTT, which is consistent with the IP determined with PESA. The MO calculations also predict that DATT has much smaller reorganization energy of hole (λ^h, 86 meV) than that of DNTT (130 meV) and BTBT (226 meV), indicating basically the same trend in the acene system, where the π-extension reduces the reorganization energies.[3] It should be also noted that the λ^h of DATT is smaller than that of pentacene (94 meV),[3] implying that DATT is promising as an organic semiconductor for OFET devices.

Packing Structure of DATT. The packing structure of DATT in the bulk crystal represents the typical molecular lamella structure (Figure 6a) with the herringbone arrangement (Figure 6b) often observed for high performance organic semiconductors for OFETs. Strictly speaking, the crystal structure of DATT is of crystallographic isostructure with that of DNTT, having the same space group ($P2_1$) and similar cell parameters,[12] and it is thus interesting to compare their intermolecular orbital overlaps. Evaluation of intermolecular electronic coupling of HOMO (transfer integral, t_{HOMO}) based on the packing structure of DATT is carried out using the Amsterdam Density Functional (ADF) program package.[24,25] The calculated t_{HOMO}s

dx.doi.org/10.1021/ja202377m |*J. Am. Chem. Soc.* 2011, 133, 8732–8739

are fairly large as expected from the π-extended molecular structure of DATT (Figure 6b). Interestingly, the values of t_{HOMO}s between the neighboring molecules are comparable to those of DNTT[12] and are well balanced for all three kinds of molecular pairs in the crystallographic *ab* cell, indicative of smaller anisotropy for DATT than for DNTT in the solid-state electronic structure. These electronic structure aspects in combination with its small λ^h values imply that DATT-based OFETs should show transport properties comparable to or even better than those of the DNTT-based ones.

Thin Film FET Devices of DATT. DATT-based thin-film OFETs were fabricated with a bottom-gate, top-contact configuration with W/L = ca. 30 on Si/SiO_2 substrates modified with various self-assembled monolayers (SAMs) and evaluated under ambient conditions. Regardless of the SAMs and substrate temperatures during deposition (T_{sub}), all of the DATT-based OFETs showed typical p-channel transistor responses. Among them, the devices fabricated on hot substrate (T_{sub} = 100 °C) demonstrated μ_{FET} values higher than 1.0 $cm^2\ V^{-1}\ s^{-1}$ and I_{on}/I_{off} values above 10^5 (Table 1). Figure 7 shows the output and transfer curves of the device fabricated on the octadecyltrichlorosilane (ODTS)-treated Si/SiO_2 substrate. In the output curves, linear increase of I_d at low V_d region, indicating the small contact resistance, is observed, likely reflecting the low IP value of DATT. Hysteresis in the transfer curves is almost negligible. As a result, the DATT-based OFETs showed characteristics comparable to those of the DNTT-based devices.[12] However, the FET characteristics of DATT-based ones largely depend on T_{sub}s, and the devices fabricated at lower T_{sub} gave inferior performances. In particular, very large T_{sub} dependence of μ_{FET} was observed for the devices fabricated on the ODTS-treated substrates (Table 1). Although the origins of the significant dependence of the ODTS-modified devices were unclear, T_{sub} dependence of μ_{FET}'s can be understood by considering that the DATT molecule is so large that it crystallizes easily at lower temperatures, resulting in difficulty in controlling the formation of well-ordered crystallites suitable for thin-film FETs. In fact, AFM images of evaporated thin films clearly support this speculation; the size of crystallites on the substrate is largely influenced by T_{sub} (Figure 8). Very small crystallites were observed in the thin film deposited at T_{sub} = rt, and upon elevating T_{sub}, the grain size increased.

Table 1. FET Characteristics of DATT Devices[a] Fabricated on Si/SiO_2 Substrates with Surface Treatments at Various Substrate Temperatures during Deposition (T_{sub})

SAM[b]	T_{sub} (°C)	μ_{FET}[c] ($cm^2\ V^{-1}\ s^{-1}$)	I_{on}/I_{off}[d]	V_{th} (V)
HMDS	rt	0.22−0.28	1×10^6	−17.4
	60	0.49−0.73	1×10^6	−12.4
	100	1.1−1.8	6×10^5	−5.0
OTS	rt	0.43−0.51	2×10^6	−14.3
	60	0.68−0.87	2×10^6	−10.7
	100	1.0−1.4	2×10^7	−4.4
ODTS	rt	$4.8-5.3 \times 10^{-2}$	5×10^5	−11.2
	60	0.23−0.26	1×10^6	−10.2
	100	2.3−3.0	5×10^5	+16.5

[a] Bottom-gate, top-contact configuration with W/L = ca. 30. [b] HMDS = hexamethyldisilazane, OTS = octyltrichlorosilane, ODTS = octadecyltrichlorosilane. [c] Data from more than 10 devices. [d] I_{on} and I_{off} were the source-drain current measured at V_g = −60 V and V_g = 0 V, respectively.

Another interesting point on the DATT-based OFETs is the threshold voltage (V_{th}) in comparison with those based on the BTBT or DNTT derivatives with different HOMO energy levels. For their reported OFETs on the Si/SiO_2 substrate showing μ_{FET} higher than 1.0 $cm^2\ V^{-1}\ s^{-1}$, the V_{th} values are −10 to −30 V for the BTBTs-based OFETs,[11] around −10 V for DNTTs-based ones,[12,16] and −5 to +16 V for the present DATT-based ones. Although the deviations are large, compounds with higher HOMO energy levels (smaller IPs) tend to have positive V_{th} values. This is in good agreement with reduction of the energy difference between the HOMO of the semiconductors and the work function (WF) of the source electrode. Shelf lifetime tests of the DATT-based OFETs in the ordinary lab conditions were also carried out (Figure S4 in Supporting Information). Although the extracted mobilities reduced slightly, no significant increase of off-current was observed.

As evidenced from their X-ray diffraction (XRD) patterns, the DATT thin films were crystalline, similar to those of DNTT thin films; clear peaks assignable to (00*l*) reflections were observed in the out-of-plane measurement (Figure 9a). Calculated interlayer spacing, 20.9 Å, is in good agreement with the crystallographic *c*-axis length of the bulk single crystal, indicating that the DATT molecules take the edge-on molecular orientation. Furthermore, appearance of peaks in the in-plane XRD (Figure 9b), all of which are also well indexed with the bulk single crystal cell, indicates its crystalline order also in the in-plane direction and the same crystalline phase both in the thin film state and the bulk single crystal.

Careful inspection of both the out-of-plane and in-plane XRDs, however, suggests that the molecular orientation of DATT in the thin film is not completely uniform; in the out-

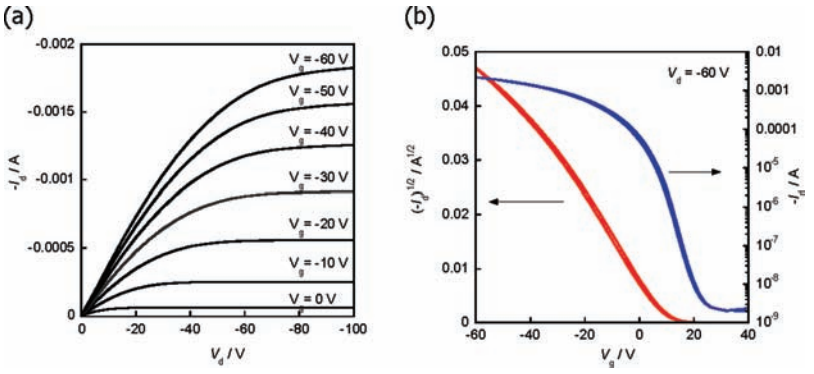

Figure 7. FET characteristics of the DATT-based device on the ODTS-treated Si/SiO_2 substrate: (a) output curves and (b) transfer curves.

dx.doi.org/10.1021/ja202377m |*J. Am. Chem. Soc.* 2011, 133, 8732–8739

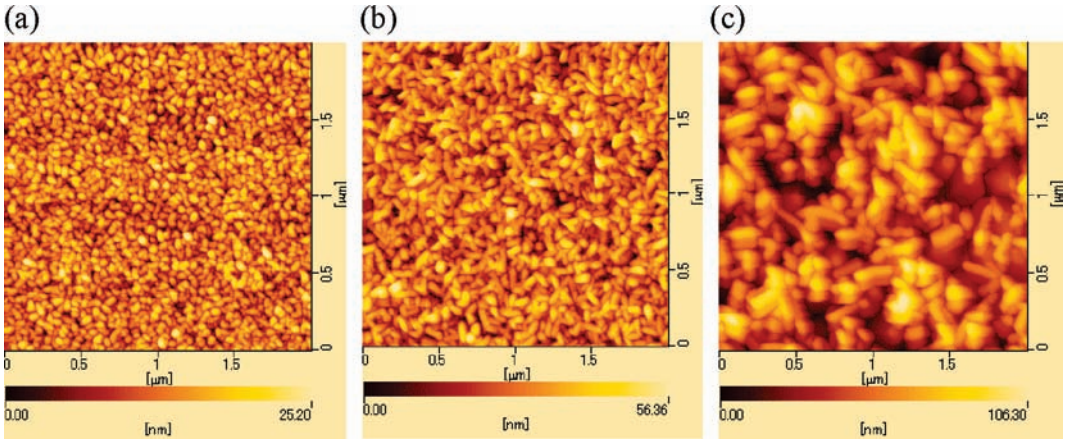

Figure 8. AFM images of evaporated thin films at various T_{sub} on ODTS-treated substrates; T_{sub} = rt (a), 60 °C (b), and 100 °C (c).

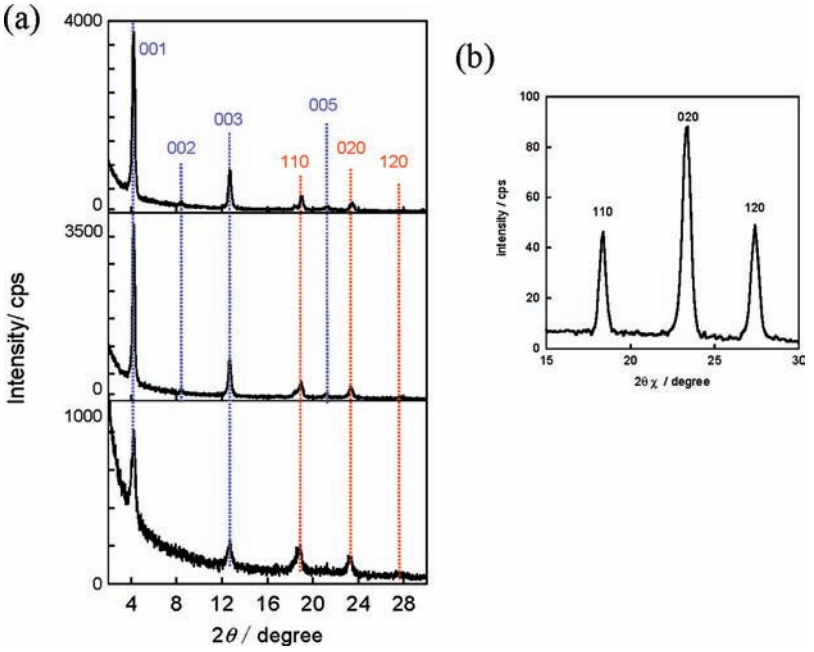

Figure 9. (a) Out-of-plane XRD patterns of DATT thin films deposited at T_{sub} = rt, 60 °C, and 100 °C from the bottom and (b) in-plane patterns (T_{sub} = 100 °C) on ODTS-treated substrates.

of-plane XRDs, there are weak but noticeable peaks assignable to the "in-plane" peaks (i.e., 110, 020, and 120), strongly indicating the existence of crystallites with the *c*-axis parallel to the substrate; in other words, crystallites with the face-on molecular orientation coexist with those with the edge-on. Such contamination of the face-on orientation is much pronounced in the thin films deposited at lower T_{sub}s (Figure 9a), which well explains the inferior FET performances of the devices fabricated at lower T_{sub}'s.[26] Even the thin film that afforded the best FET performances ($\mu \approx 3.0$ cm^2 V^{-1} s^{-1}) shows the "in-plane" peaks in the out-of-plane XRD (Figure 9a, top), indicating the existence of the face-on phase that would limit the FET performances. Thus, much better transport characteristics can be expected, provided that improvement of molecular ordering in the thin film state of the DATT-based devices by optimizing film deposition conditions and/or derivatization of the DATT molecule are possible.

CONCLUSION

In summary, we have successfully developed DATT, a new π-extended ladder-type compound with eight fused aromatic rings. Even with its highly extended acene-like π-system, DATT is a fairly air-stable compound with IP of 5.1 eV. A field-effect mobility as high as 3.0 cm^2 V^{-1} s^{-1} was achieved with vapor-processed DATT-based devices, even though the thin-film ordering is not very good. Therefore, improvement of molecular ordering by optimizing the film deposition conditions and derivatization of DATT could further improve the performances. In the latter context, the synthetic method newly developed is quite suitable to synthesize DATT derivatives and its related largely π-extended heteroarenes, since the method is highly selective and efficient starting from readily available methoxy-substituted aromatic compounds. Thus, design, synthesis, and evaluation of new largely extended compounds are now underway in our group.

dx.doi.org/10.1021/ja202377m |*J. Am. Chem. Soc.* 2011, 133, 8732–8739

EXPERIMENTAL SECTION

General. All chemicals and solvents are of reagent grade unless otherwise indicated. THF was purified with a standard distillation procedure prior to use. 2-Methoxyanthracene (**4**)[20] was synthesized as reported. Melting points were uncorrected. All reactions were carried out under nitrogen atmosphere. Nuclear magnetic resonance (NMR) spectra were obtained in deuterated chloroform ($CDCl_3$) with TMS as internal reference unless otherwise stated; chemical shifts (δ) are reported in parts per million. IR spectra were recorded using a KBr pellet for solid samples. EI-MS spectra were obtained using an electron impact ionization procedure (70 eV).

3-Methylthio-2-methoxyanthracene (5). To a solution of 2-methoxyanthracene (**4**, 15.0 g, 72 mmol) in THF (520 mL) was added 1.67 M hexane solution of *n*-BuLi (86 mL, 144 mmol) at 0 °C. After the mixture was stirred for 1 h at room temperature, dimethyldisulfide (13 mL, 150 mmol) was added to the solution at 0 °C, and the resulting mixture was stirred for 7 h at room temperature. The mixture was poured into water (100 mL), and then THF was evaporated in vacuo to give a precipitate. The precipitate was collected by filtration and washed with water (100 mL) and methanol (100 mL) to give 3-methylthio-2-methoxyanthracene (18.3 g, quantitative yield) as a white solid. An analytical sample was obtained by gel-permeation chromatography with JAI-GEL 1H/2H column assembly. Colorless crystals; mp 176.5−177.5 °C; ^{1}H NMR (400 MHz, $CDCl_3$) δ 2.58 (s, 3H), 4.03 (s, 3H), 7.16 (s, 1H), 7.39 (ddd, J = 8.2, 4.9, 1.9 Hz, 1H), 7.42 (ddd, J = 8.2, 4.9, 1.9 Hz, 1H), 7.55 (s, 1H), 7.92 (d, J = 9.5 Hz, 1H) 7.93 (d, J = 9.5 Hz, 1H), 8.22 (s, 1H), 8.24 (s, 1H); ^{13}C NMR (125 MHz, $CDCl_3$) δ 14.7, 56.2, 103.4, 122.5, 124.3, 124.7, 124.9, 125.4, 127.9, 128.4, 128.9, 131.0, 131.0, 131.7, 131.8, 154.6; EIMS (70 eV) m/z = 254 (M^+). Anal. Calcd for $C_{16}H_{14}OS$: C, 75.55; H, 5.55. Found: C, 75.26; H, 5.33.

3-(Methylthio)anthracen-2-ol. To a solution of 3-methylthio-2-methoxyanthracene (**5**, 14.5 g, 57 mmol) in dichloromethane (200 mL) was added dropwise a dichloromethane solution of BBr_3 (ca. 2 M, 50 mL, 100 mmol) at −78 °C. After 5 h of stirring at room temperature, ice (ca. 50 g) was added to the mixture at 0 °C. The resulting mixture was extracted with dichloromethane (200 mL × 3), and the combined organic layer was washed with brine (100 mL × 3), dried ($MgSO_4$), and concentrated in vacuo to give practically pure 3-(methylthio) anthracen-2-ol (13.7 g, quantitative yield) as a white solid. An analytical sample was obtained by gel-permeation chromatography with JAI-GEL 1H/2H column assembly. Colorless crystals; mp 175.6−176.5 °C; ^{1}H NMR (400 MHz, $CDCl_3$) δ 2.49 (s, 3H), 6.54 (s, 1H), 7.31 (s, 1H), 7.39 (ddd, J = 10.7, 6.6, 1.4 Hz, 1H), 7.41 (s, 1H), 7.43 (ddd, J = 10.7, 6.6, 1.4 Hz, 1H), 7.91 (d, J = 8.8 Hz, 1H), 7.93 (dd, J = 8.8 Hz, 1H), 8.14 (s, 1H), 8.22 (s, 1H), 8.30 (s, 1H); ^{13}C NMR (100 MHz, $CDCl_3$) δ 19.8, 107.8, 124.2, 125.0, 126.2, 126.2, 126.8, 128.0, 128.5, 128.6, 130.8, 132.8, 133.0, 133.8, 151.7; IR (KBr) ν 3510 cm^{-1} (OH); EIMS (70 eV) m/z = 240 (M^+). Anal. Calcd for $C_{15}H_{12}OS$: C, 74.66; H, 4.72. Found: C, 74.70; H, 4.84.

3-(Methylthio)anthracen-2-yl Trifluoromethanesulfonate (6). To a solution of 3-(methylthio)anthracen-2-ol (10.1 g, 42 mmol) and triethylamine (16.0 mL, 115 mmol) in dichloromethane (400 mL) was added trifluoromethanesulfonic anhydride (10.0 mL, 54.6 mmol) at 0 °C. After 42 h of stirring at room temperature, the mixture was diluted with water (50 mL) and hydrochloric acid (4 M, 100 mL). The resulting mixture was extracted with dichloromethane (100 mL × 3). The combined organic layer was washed with brine (100 mL × 3), dried ($MgSO_4$), and concentrated in vacuo to give practically pure 3-(methylthio)anthracen-2-yl trifluoromethanesulfonate (15.5 g, quantitative yield) as a yellow solid. An analytical sample was obtained by gel-permeation chromatography with JAI-GEL 1H/2H column assembly. Colorless crystals; mp 105.5−106.0 °C; ^{1}H NMR (400 MHz, $CDCl_3$) δ 2.63 (s, 3H), 7.50 (ddd, J = 9.6, 6.3, 1.8 Hz, 1H), 7.51 (ddd, J = 9.6, 6.3, 1.8 Hz, 1H), 7.78 (s, 1H), 7.88 (s, 1H), 7.97 (dd, J = 5.5, 2.0 Hz, 1H), 7.98 (dd, J = 5.5, 2.0 Hz, 1H), 8.34 (s, 1H), 8.38 (s, 1H); ^{13}C NMR (125 MHz, $CDCl_3$) δ 15.8, 119.0 (q, J = 319 Hz), 119.5, 125.4, 126.2, 126.4, 126.8, 127.1, 128.4 (×2), 129.0, 130.6, 131.0, 132.0, 132.9, 145.3; IR (KBr) ν 1429, 1207 cm^{-1} (-O-SO_2-); EIMS (70 eV) m/z = 372 (M^+). Anal. Calcd for $C_{16}H_{11}F_3O_3S_2$: C, 51.61; H, 2.98. Found C, 51.57; H, 2.67.

***trans*-1,2-Bis(3-methylthioanthracen-2-yl)ethene (3).** To a deaerated solution of 3-(methylthio)anthracen-2-yl trifluoromethanesulfonate (**6**, 11.2 g, 30 mmol) and *trans*-1,2-bis(tributylstannyl)ethane[21] (9.1 g, 15.0 mmol) in DMF (110 mL) was added $Pd(PPh_3)_4$ (1.2 g, 1.0 mmol, 3 mol %). The mixture was heated at 100 °C for 17 h in dark and then diluted with water. The resulting precipitate was collected by filtration and washed with water (100 mL) and ethanol (50 mL) to give practically pure *trans*-1,2-bis(3-methylthioanthracen-2-yl)ethene (3.9 g, 59%) as a yellow solid. An analytical sample was obtained by vacuum sublimation. Mp > 300 °C; ^{1}H NMR (400 MHz, $CDCl_3$) δ 2.66 (s, 6H), 7.44 (dd, J = 5.0, 4.4 Hz, 4H), 7.75 (s, 2H), 7.78 (s, 2H), 7.97 (d, J = 9.6 Hz, 2H), 7.98 (d, J = 9.6 Hz, 2H), 8.27 (s, 2H), 8.30 (s, 2H), 8.44 (s, 2H); ^{13}C NMR (100 MHz, $CDCl_3$) δ 16.8, 124.2, 124.9, 125.7, 125.7, 126.0, 126.8, 126.9, 128.5, 128.6, 129.2, 130.6, 132.0, 132.8, 136.5, 147.3; IR (KBr) ν 1485, 1426, 1024, 957, 862, 741 cm^{-1}; EIMS (70 eV) m/z = 472 (M^+).; Anal. Calcd for $C_{32}H_{24}S_2$: C, 81.31; H, 5.12. Found: C, 81.21; H, 4.90.

Dianthra[2,3-*b*:2′,3′-*f*]thieno[3,2-*b*]thiophene (DATT). Powdered iodine (59 g, 232 mmol) was added to a suspension of *trans*-1,2-bis(3-methylthioanthracen-2-yl)ethene (3.8 g, 8.0 mmol) in acetic acid (250 mL), and the mixture was refluxed for 11 h. Excess acetic acid was distilled off, and the resulting residue was treated with saturated aqueous sodium hydrogen sulfite solution (200 mL) with stirring (ca. 1 h). The resulting precipitate was collected by filtration, washed successively with water (100 mL) and acetone (100 mL), and dried in vacuo to give crude DATT (3.8 g, quantitative) as a dark reddish solid. For device fabrication, the crude DATT was washed with boiling chlorobenzene and then purified by repetitive gradient sublimation in vacuo (ca. 400 °C at ∼10^{-2} Pa under nitrogen atmosphere), which gave typically 50% yield of purified DATT with sufficient quality. Mp > 300 °C; EIMS (70 eV) m/z = 440 (M^+). Anal. Calcd for $C_{30}H_{16}S_2$: C, 81.78; H, 3.66. Found: C, 81.38; H, 3.52.

Single Crystal X-ray Analysis. Single crystals of DATT for X-ray structural analysis were obtained by a sublimation method. The X-ray crystal structure analysis was made on a Rigaku Mercury-CCD (Mo Kα radiation, λ = 0.71069 Å, graphite monochromator, T = 296 K, $2\theta_{max}$ = 55.0°). The structure was solved by the direct methods.[27] Non-hydrogen atoms were refined anisotropically, and hydrogen atoms were included in the calculations but not refined. All calculations were performed using the crystallographic software package TeXsan 1.2.[28]

Crystallographic data for DATT: $C_{30}H_{16}S_2$ (440.58), orange plate, 0.30 × 0.20 × 0.10 mm^3, monoclinic, space group, $P2_1$ (No. 4), a = 6.259(3), b = 7.569(3), c = 20.826(9) Å, b = 92.781(1)°, V = 985.3(7) Å^3, Z = 2, R = 0.0595 for 3127 observed reflections ($I > 2\sigma(I)$) and 289 variable parameters, wR^2 = 0.1473 for all data (3563).

Fabrication and Evaluation of FET Devices. OFETs were fabricated in a "top-contact" configuration on a heavily doped n^+-Si (100) wafer with a 200 nm thermally grown SiO_2 (C_i = 17.3 nF cm^{-2}). The substrate surfaces were treated with octyltrichlorosilane (OTS), octadecyltrichlorosilane (ODTS), or hexamethyldisilazane (HMDS) as reported previously. A thin film of DATT as the active layer was vacuum-deposited on the Si/SiO_2 substrates maintained at various temperatures (T_{sub}) at a rate of 1 Å s^{-1} under a pressure of ∼10^{-3} Pa. On top of the organic thin film, gold films (80 nm) as drain and source electrodes were deposited through a shadow mask. For a typical device, the drain-source channel length (L) and width (W) are 50 μm and 1.5 mm, respectively. Characteristics of the OFET devices were measured at room temperature under ambient conditions with a Keithley 4200 semiconducting

parameter analyzer. Field-effect mobility (μ_{FET}) was calculated in the saturation ($V_d = -60$ V) of the I_d using the following equation,

$$I_d = C_i \mu_{FET} (W/2L)(V_g - V_{th})^2$$

where C_i is the capacitance of the SiO_2 insulator, and V_g and V_{th} are the gate and threshold voltages, respectively. Current on/off ratio (I_{on}/I_{off}) was determined from the I_d at $V_g = 0$ V (I_{off}) and $V_g = -60$ V (I_{on}). The μ_{FET} data reported are typical values from more than ten different devices.

Theoretical Calculations. Geometry optimizations and normal mode calculations of isolated nTA molecules of BTBT, DNTT, and DATT were performed at the B3LYP/6-31G(d) level using the Gaussian03 program package. Reorganization energies of hole were also calculated using the same program package at the same level following the procedures described in ref 3. Calculations of intermolecular transfer integrals (t's) were performed with the PW91 functional and Slater-type triple-ζ plus polarization (TZP) basis sets using the ADF (Amsterdam Density Functional) package.[24,25]

■ ASSOCIATED CONTENT

Supporting Information. Crystallographic data in CIF format for DATT, DSC trace of DATT, shelf lifetime test of DATT-based OFET, complete ref 23, and NMR spectra of the synthetic intermediates. This material is available free of charge via the Internet at http://pubs.acs.org.

■ AUTHOR INFORMATION

Corresponding Author
ktakimi@hiroshima-u.ac.jp

■ ACKNOWLEDGMENT

This work was partially supported by a Grant-in-Aid for Scientific Research (No. 20350088 and 23245041) from the Ministry of Education, Culture, Sports, Science and Technology, Japan and Founding Program for World-Leading R&D on Science and Technology (FIRST), Japan.

■ REFERENCES

(1) (a) Rogers, J. A.; Bao, Z.; Katz, H. E.; Dodabalapur, A. In *Thin-Film Transistors*; Kagan, C. R., Andry, P., Eds.; Marcel Dekker: New York, 2003; p 377. (b) *Organic Electronics, Manufacturing and Applications*; Klauk, H., Ed.; Wiley-VCH: Weinheim, 2006. (c) *Organic Field-Effect Transistors*; Bao, Z., Locklin, J., Eds.; CRC Press: Boca Raton, 2007. (d) Facchetti, A. *Mater. Today* **2007**, *10*, 28–37. (e) Anthony, J. E.; Facchetti, A.; Heeney, M.; Marder, S. R.; Zhan, X. *Adv. Mater.* **2010**, *22*, 3876–3892. (f) Jung, B. J.; Tremblay, N. J.; Yeh, M.-L.; Katz, H. E. *Chem. Mater.* **2011**, *23*, 568–582. (g) Facchetti, A. *Chem. Mater.* **2011**, *23*, 733–758.

(2) Lee, S.; Koo, B.; Shin, J.; Lee, E.; Park, H.; Kim, H. *Appl. Phys. Lett.* **2006**, *88*, 162109.

(3) (a) Bredas, J.-L.; Beljonne, D.; Coropceanu, V.; Cornil, J. *Chem. Rev.* **2004**, *104*, 4971–5004. (b) Coropceanu, V.; Kwon, O.; Wex, B.; Kaafarani, B. R.; Gruhn, N. E.; Durivage, J. C.; Neckers, D. C.; Bredas, J.-L. *Chem.—Eur. J.* **2006**, *12*, 2073–2080. (c) Valiyev, F.; Hu, W.-S.; Chen, H.-Y.; Kuo, M.-Y.; Chao, I.; Tao, Y.-T. *Chem. Mater.* **2007**, *19*, 3018–3026.

(4) Maliakal, A.; Raghavachari, K.; Katz, H.; Chandross, E.; Siegrist, T. *Chem. Mater.* **2004**, *16*, 4980–4986.

(5) Payne, M. M.; Parkin, S. R.; Anthony, J. E. *J. Am. Chem. Soc.* **2005**, *127*, 8028–8029.

(6) Mondal, R.; Adhikari, R. M.; Shah, B. K.; Neckers, D. C. *Org. Lett.* **2007**, *9*, 2505–2508.

(7) Payne, M. M.; Odom, S. A.; Parkin, S. R.; Anthony, J. E. *Org. Lett.* **2004**, *6*, 3325–3328.

(8) (a) Zhang, X.; Côté, A. P.; Matzger, A. J. *J. Am. Chem. Soc.* **2005**, *127*, 10502–10503. (b) Okamoto, T.; Kudoh, K.; Wakamiya, A.; Yamaguchi, S. *Chem.—Eur. J.* **2007**, *13*, 548–556.

(9) (a) Sirringhaus, H.; H. Friend, R.; Wang, C.; Leuninger, J.; Mullen, K. *J. Mat. Chem.* **1999**, *9*, 2095–2101. (b) Gao, P.; Feng, X.; Yang, X.; Enkelmann, V.; Baumgarten, M.; Mullen, K. *J. Org. Chem.* **2008**, *73*, 9207–9213. (c) Gao, P.; Cho, D.; Yang, X.; Enkelmann, V.; Baumgarten, M.; Müllen, K. *Chem.—Eur. J.* **2010**, *16*, 5119–5128.

(10) Yamada, K.; Okamoto, T.; Kudoh, K.; Wakamiya, A.; Yamaguchi, S.; Takeya, J. *Appl. Phys. Lett.* **2007**, *90*, 072102.

(11) (a) Takimiya, K.; Ebata, H.; Sakamoto, K.; Izawa, T.; Otsubo, T.; Kunugi, Y. *J. Am. Chem. Soc.* **2006**, *128*, 12604–12605. (b) Ebata, H.; Izawa, T.; Miyazaki, E.; Takimiya, K.; Ikeda, M.; Kuwabara, H.; Yui, T. *J. Am. Chem. Soc.* **2007**, *129*, 15732–15733. (c) Izawa, T.; Miyazaki, E.; Takimiya, K. *Adv. Mater.* **2008**, *20*, 3388–3392.

(12) (a) Yamamoto, T.; Takimiya, K. *J. Am. Chem. Soc.* **2007**, *129*, 2224–2225. (b) Yamamoto, T.; Takimiya, K. *J. Photopolym. Sci. Technol.* **2007**, *20*, 57–59. (c) Yamamoto, T.; Shinamura, S.; Miyazaki, E.; Takimiya, K. *Bull. Chem. Soc. Jpn.* **2010**, *83*, 120–130.

(13) (a) Uno, M.; Tominari, Y.; Takeya, J. *Appl. Phys. Lett.* **2008**, *93*, 173301. (b) Kano, M.; Minari, T.; Tsukagoshi, K. *Appl. Phys. Lett.* **2009**, *94*, 143304. (c) Minari, T.; Kano, M.; Miyadera, T.; Wang, S.-D.; Aoyagi, Y.; Tsukagoshi, K. *Appl. Phys. Lett.* **2009**, *94*, 093307. (d) Uemura, T.; Hirose, Y.; Uno, M.; Takimiya, K.; Takeya, J. *Appl. Phys. Express* **2009**, *2*, 111501. (e) Endo, T.; Nagase, T.; Kobayashi, T.; Takimiya, K.; Ikeda, M.; Naito, H. *Appl. Phys. Express* **2010**, *3*, 121601. (f) Kano, M.; Minari, T.; Tsukagoshi, K. *Appl. Phys. Express* **2010**, *3*, 051601. (g) Liu, C.; Minari, T.; Lu, X.; Kumatani, A.; Takimiya, K.; Tsukagoshi, K. *Adv. Mater.* **2011**, *23*, 523–526. (h) Iino, H.; Hanna, J.-i. *Adv. Mater.* **2011**, *23*, 1748–1751.

(14) (a) Uno, M.; Doi, I.; Takimiya, K.; Takeya, J. *Appl. Phys. Lett.* **2009**, *94*, 103307. (b) Zschieschang, U.; Ante, F.; Yamamoto, T.; Takimiya, K.; Kuwabara, H.; Ikeda, M.; Sekitani, T.; Someya, T.; Kern, K.; Klauk, H. *Adv. Mater.* **2010**, *22*, 982–985. (c) Uno, M.; Hirose, Y.; Uemura, T.; Takimiya, K.; Nakazawa, Y.; Takeya, J. *Appl. Phys. Lett.* **2010**, *97*, 013301. (d) McCarthy, M. A.; Liu, B.; Rinzler, A. G. *Nano Lett.* **2010**, *10*, 3467–3472. (e) Zschieschang, U.; Yamamoto, T.; Takimiya, K.; Kuwabara, H.; Ikeda, M.; Sekitani, T.; Someya, T.; Klauk, H. *Adv. Mater.* **2011**, *23*, 654–658.

(15) Uno, M.; Tominari, Y.; Yamagishi, M.; Doi, I.; Miyazaki, E.; Takimiya, K.; Takeya, J. *Appl. Phys. Lett.* **2009**, *94*, 223308.

(16) (a) Kang, M. J.; Doi, I.; Mori, H.; Miyazaki, E.; Takimiya, K.; Ikeda, M.; Kuwabara, H. *Adv. Mater.* **2011**, *23*, 1222–1225. (b) Nakayama, K.; Hirose, Y.; Soeda, J.; Yoshizumi, M.; Uemura, T.; Uno, M.; Li, W.; Kang, M. J.; Yamagishi, M.; Okada, Y.; Miyazaki, E.; Nakazawa, Y.; Nakao, A.; Takimiya, K.; Takeya, J. *Adv. Mater.* **2011**, *23*, 1626–1629.

(17) (a) Takimiya, K.; Yamamoto, T.; Ebata, H.; Izawa, T. *Sci. Technol. Adv. Mater.* **2007**, *8*, 273–276. (b) Sanchez-Carrera, R. S.; Atahan, S.; Schrier, J.; Aspuru-Guzik, A. *J. Phys. Chem. C* **2010**, *114*, 2334–2340.

(18) Gore, P. H. *J. Chem. Soc* **1959**, 1616–1618.

(19) Although the synthesis of DATT with the same route was described, no detailed characterization of either DATT nor the intermediates was reported. Aspuru-Guzik, A.; Schrier, J.; Granados-Focil, S.; Coughlin, E. B., PCT Int. Appl. (2009), WO 2009009790 A1 20090115.

(20) Labadie, G. R.; Cravero, R. M. *Chem. Educ.* **1999**, *4*, 219–220.

(21) (a) Bottaro, J. C.; Hanson, R. N.; Seitz, D. E. *J. Org. Chem.* **1981**, *46*, 5221–5222. (b) Haack, R. A.; Penning, T. D.; Djuric, S. W.; Dziuba, J. A. *Tetrahedron Lett.* **1988**, *29*, 2783–2786.

(22) Usta, H.; Risko, C.; Wang, Z.; Huang, H.; Deliomeroglu, M. K.; Zhukhovitskiy, A.; Facchetti, A.; Marks, T. J. *J. Am. Chem. Soc.* **2009**, *131*, 5586–5608.

(23) MO calculations were carried out with the DFT/TD-DFT method at the B3LYP/6-31g(d) level using Gaussian 03 program

package. Frisch, M. J. *Gaussian 03*, revision C.02; Gaussian, Inc.: Wallingford, CT, 2004.

(24) *ADF2008.01*; SCM, Theoretical Chemistry, Vrije Universiteit: Amsterdam, The Netherlands; http://www.scm.com.

(25) (a) Senthilkumar, K.; Grozema, F. C.; Bickelhaupt, F. M.; Siebbeles, L. D. A. *J. Chem. Phys.* **2003**, *119*, 9809–9817. (b) Prins, P.; Senthilkumar, K.; Grozema, F. C.; Jonkheijm, P.; Schenning, A. P. H. J.; Meijer, E. W.; Siebbeles, L. D. A. *J. Phys. Chem. B* **2005**, *109*, 18267–18274.

(26) Christos, D.; Dimitrakopoulos, C. D.; Malenfant, P. R. L. *Adv. Mater.* **2002**, *14*, 99–117.

(27) Sheldrick, G. M. *SHELXL (SHELX97)*, Programs for the refinement of crystal structures; University of Goettingen: Germany, 1997.

(28) *teXsan: Single Crystal Structure Analysis Software*, Version 1.2; Molecular Structure Corporation and Rigaku Corporation: The Woodlands, TX, 2000.